JCB Article

Two ZBP1 KH domains facilitate β-actin mRNA localization, granule formation, and cytoskeletal attachment

Kim L. Farina,[1] Stefan Hüttelmaier,[1] Kiran Musunuru,[2,3] Robert Darnell,[3,4] and Robert H. Singer[1]

[1]Department of Anatomy and Structural Biology, Albert Einstein College of Medicine, Bronx, NY 10461
[2]Laboratory of Molecular Biophysics and [3]Laboratory of Molecular Neuro-Oncology, [4]Howard Hughes Medical Institute, The Rockefeller University, New York, NY 10021

Chicken embryo fibroblasts (CEFs) localize β-actin mRNA to their lamellae, a process important for the maintenance of cell polarity and motility. The localization of β-actin mRNA requires a cis localization element (zipcode) and involves zipcode binding protein 1 (ZBP1), a protein that specifically binds to the zipcode. Both localize to the lamellipodia of polarized CEFs. ZBP1 and its homologues contain two NH_2-terminal RNA recognition motifs (RRMs) and four COOH-terminal hnRNP K homology (KH) domains. By using ZBP1 truncations fused to GFP in conjunction with in situ hybridization analysis, we have determined that KH domains three and four were responsible for granule formation and cytoskeletal association. When the NH_2 terminus was deleted, granules formed by the KH domains alone did not accumulate at the leading edge, suggesting a role for the NH_2 terminus in targeting transport granules to their destination. RNA binding studies were used to show that the third and fourth KH domains, not the RRM domains, bind the zipcode of β-actin mRNA. Overexpression of the four KH domains or certain subsets of these domains delocalized β-actin mRNA in CEFs and inhibited fibroblast motility, demonstrating the importance of ZBP1 function in both β-actin mRNA localization and cell motility.

Introduction

One mechanism used by polarized cells to establish and maintain their asymmetry is localization of transcripts to specific subcellular locations (for review see Kloc et al., 2002). The phenomenon of RNA localization has been observed in oocytes and developing embryos of *Drosophila* and *Xenopus* (Bashirullah et al., 1998; King et al., 1999; Mowry and Cote, 1999; Lasko, 2000) in yeast (Long et al., 1997) and in somatic cells such as fibroblasts and neurons (Lawrence and Singer, 1986; Steward, 1997). β-Actin mRNA is localized at the leading lamellae of chicken embryo fibroblasts (CEFs) (Lawrence and Singer, 1986) and at the growth cone of developing neurons (Bassell et al., 1998). The localization of β-actin mRNA is dependent on the zipcode, a 54 nt cis-acting element located in the 3′ UTR of the mRNA (Kislauskis et al., 1993). Treatment with antisense oligonucleotides to this element delocalizes the mRNA and results in impaired cell polarity and motility (Kislauskis et al., 1994, 1997; Shestakova et al., 1999). The trans-acting factor, zipcode binding protein 1 (ZBP1),* was affinity purified with the zipcode of β-actin mRNA and subsequently cloned (Ross et al., 1997). ZBP1 is a predominantly cytoplasmic protein that binds directly to the zipcode of β-actin mRNA and colocalizes with the mRNA to the leading lamellae of CEFs (Ross et al., 1997; Oleynikov and Singer, 2003) and to the neuronal growth cone (Zhang et al., 2001a). In neurons, neurotrophin-stimulated increases in β-actin mRNA levels and growth cone formation depend on the formation of a complex involving both β-actin mRNA and ZBP1 (Zhang et al., 1999a, 2001a).

After the identification of ZBP1, additional homologues were identified in a wide range of organisms including *Xenopus*, *Drosophila*, human, and mouse (Mueller-Pillasch et al., 1997; Deshler et al., 1998; Doyle et al., 1998; Havin et al., 1998; Nielsen et al., 1999, 2000; Zhang et al., 1999b). ZBP1 family members are expressed in germ line cells of *Drosophila* and *Xenopus* and in embryonic fibroblasts and

Address correspondence to Robert H. Singer, Dept. of Anatomy and Structural Biology, Albert Einstein College of Medicine, 1300 Morris Park Ave., Bronx, NY 10461. Tel.: (718) 430-8646. Fax: (718) 430-8697. E-mail: rhsinger@aecom.yu.edu

Key words: RNA localization; RNA binding protein; KH domain protein; cell motility; CRD-BP

*Abbreviations used in this paper: CEF, chick embryo fibroblast; DEPC, diethylpyrocarbonate; KH, hnRNP K homology; RRM, RNA recognition motif; ZBP1, zipcode binding protein 1; ΔZBP1, truncated ZBP1.

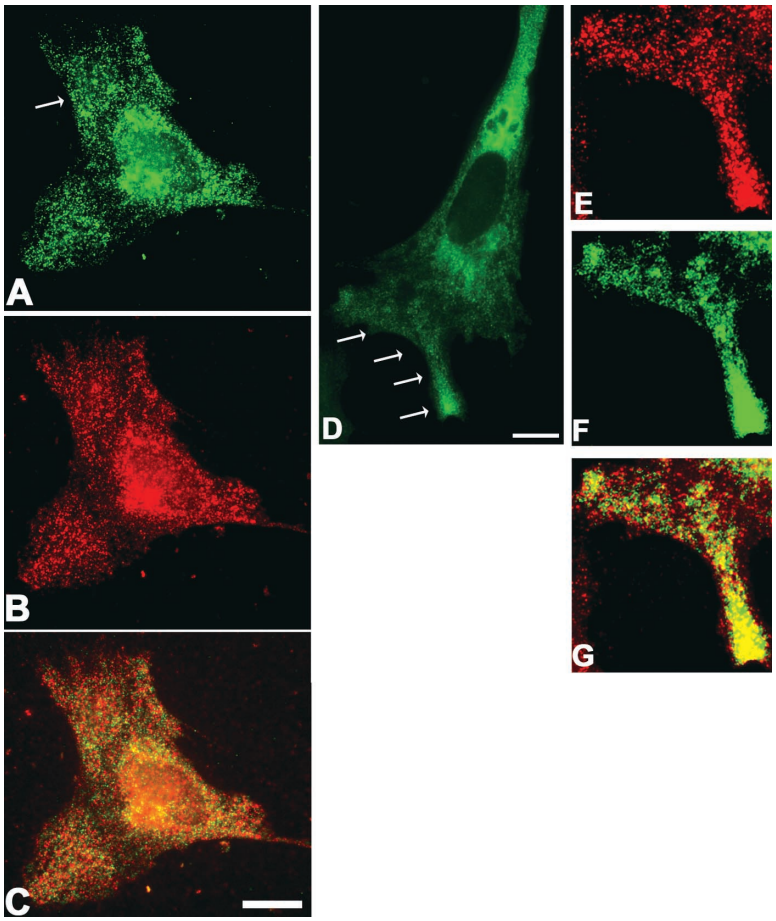

Figure 1. **Distribution of β-actin mRNA and ZBP1 in CEFs.** ZBP1 localizes in granular structures (arrow) that, along with β-actin mRNA, are enriched in cell lamellae. Immunofluorescence of ZBP1 (A) and in situ hybridization of β-actin mRNA (B) in serum-stimulated CEFs. (C) Overlap of A and C. CEFs were transiently transfected with GFP-tagged ZBP1 (D) and subsequently hybridized with β-actin mRNA fluorescent oligonucleotide (E). GFP–ZBP1 forms granules that are enriched at the cell periphery. Partial masking of granules is occurring due to high signal intensities. The enlargements (3×) (E–G) of indicated region in D (arrows) demonstrate a spatial overlap (G) of β-actin probe (E) and GFP–ZBP1 (F) within the cell protrusion. Bars, 10 μm.

neurons. ZBP1-like proteins contain two RNA recognition motifs (RRMs) at the NH_2-terminal part of the protein and four COOH-terminal hnRNP K homology (KH) domains at the COOH-terminal end. ZBP1 family members are implicated in numerous aspects of RNA regulation: stability (Leeds et al., 1997), translation (Nielsen et al., 1999), and localization (Deshler et al., 1997, 1998; Ross et al., 1997; Havin et al., 1998). In addition, they are overexpressed in several types of cancer (Mueller-Pillasch et al., 1997; Zhang et al., 1999b, 2001b). However, their role as trans-acting factors in RNA localization has not been well established.

ZBP1 appears in large cytoplasmic granules that are codistributed with β-actin mRNA granules in the cytoplasm of CEFs. Granule formation is typical of localized mRNAs. Messenger RNA-containing granules (mRNP) are thought to contain components necessary for transport, localization, and translation of specific mRNAs (Barbarese et al., 1995). We propose that in CEFs granule formation depends on interactions of ZBP1 with the β-actin mRNA zipcode and that localization is dependent on mRNP formation. In addition, β-actin mRNA localization in fibroblasts is important for the maintenance of cell polarity and motility (Kislauskis et al., 1994, 1997; Shestakova et al., 2001). Based on this, we reasoned that ZBP1 interactions with β-actin mRNA might also be influencing CEF motility.

Here we present an extensive functional characterization of ZBP1. We have used scanning deletion mutagenesis of ZBP1 to identify functionally important regions. Specifically, we used these constructs to determine polypeptide chain segments responsible for granule formation, granule localization, cytoskeleton association, and RNA binding. We show that the two COOH-terminal KH domains of ZBP1 are sufficient for zipcode binding, granule formation, and cytoskeletal retention on microfilaments; functions that ultimately lead to the localization of the RNA. The NH_2 terminus of the protein is necessary for localization of ZBP1-containing granules. We also demonstrate a physiological consequence of impairing ZBP1 function by showing that either overexpression of ZBP1 or a β-actin mRNA-delocalizing truncation of ZBP1 decreases cell motility.

Results

ZBP1 forms granules that are enriched at the periphery of CEFs

The subcellular distribution of ZBP1 was analyzed in CEFs using rabbit antiserum prepared against recombinant full-length ZBP1. In CEFs, endogenous ZBP1 localizes in granular structures that are enriched within lamellipodia, the perinucleus, and the retracting tail (Fig. 1 A). The lamellar distribution of ZBP1 mimics that of β-actin mRNA (Fig. 1, A–C).

The localization pattern of GFP–ZBP1 was compared with endogenous ZBP1 in CEFs after transfection with GFP–ZBP1. In CEFs, overexpressed GFP–ZBP1 formed

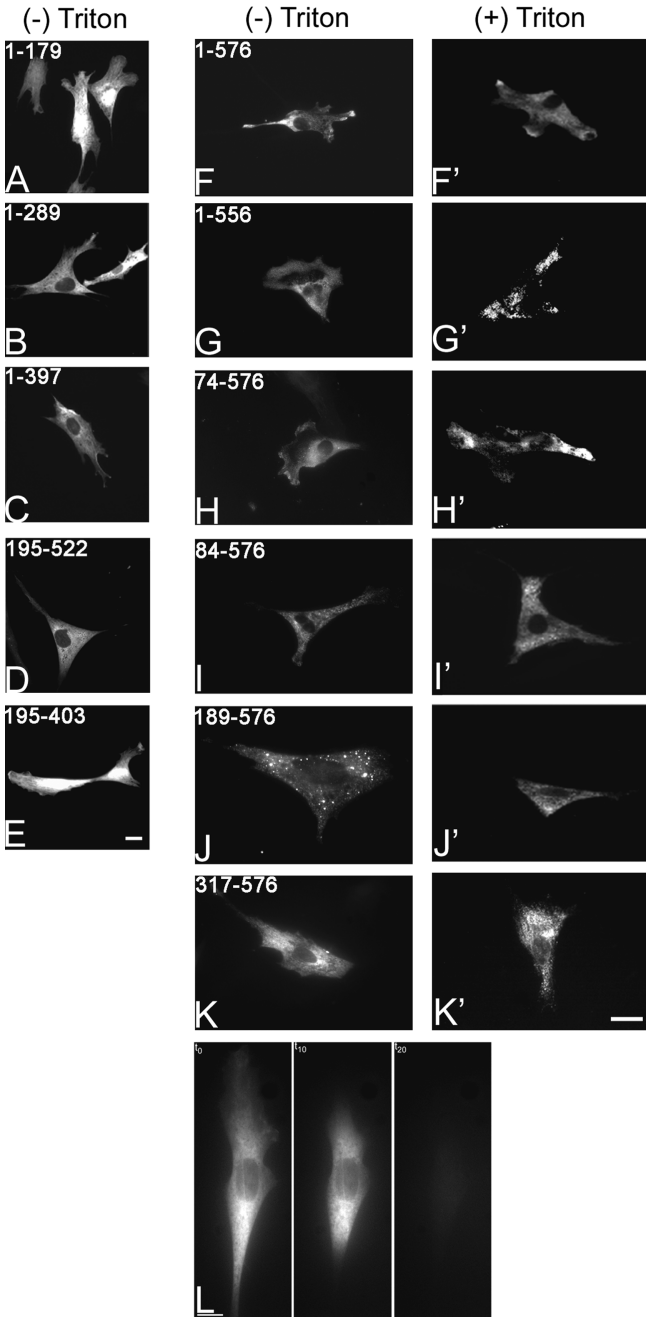

Figure 2. **Cytoplasmic granule formation and cytoskeletal anchoring is mediated by KH3-KH4 of ZBP1.** ZBP1 fragments fused to GFP were transiently transfected into CEFs. Localization of GFP-tagged proteins was analyzed before (A–J) and after (F′–J′) extraction with Triton X-100. (A–E) Note that all protein fragments lacking the two COOH-terminal KH domains (KH3 and KH4) in their entirety were evenly distributed throughout the cytoplasm (A, 1–179; B, 1–289; C, 1–397; D, 195–522; E, 195–403) and no granular structures were observed. All of these fusion proteins were extracted from the cytoplasm by treatment with Triton X-100 before fixation (L). (F–K) CEFs transiently transfected with: F, 1–576; G, 1–556; H, 74–576; I, 84–576; J, 189–576; and K, 317–576. The NH_2-terminal truncated fragments formed large granules that were resistant to detergent extraction. The left column (F–J) shows nonextracted fixed cells. Cells in the right column (F′–J′) have been Triton extracted. Note that granules formed by constructs in G (1–556) and H (74–576) are enriched in the lamellae, whereas granules formed by the remaining constructs, I (84–576), J (189–576), and K (317–576), were evenly distributed in the cytoplasm. (L) To demonstrate the loss of COOH-terminal truncated GFP fusion proteins by extraction, the loss of GFP signal was visualized after the introduction of Triton X-100 (t_0). The COOH-terminal truncated fragment (1–397) was initially diffusely distributed in the cytoplasm. No significant signal was detected after 20 s of Triton extraction. Images shown are at introduction of Triton X-100 (t_0), 10 s post-Triton (t_{10}), and 20 s post-Triton (t_{20}). Bars, 10 μm.

large cytoplasmic granules (Fig. 1 D) similar to those formed by endogenous ZBP1 (Fig. 1 A). Granules were enriched at cell protrusions, the perinuclear region, and the retracting tail of the cells. Like endogenous ZBP1, GFP–ZBP1 granules were resistant to cytoplasmic extraction with Triton X-100, indicating that they maintained stable interactions with the cytoskeleton (Fig. 2 F′).

Codistribution of GFP–ZBP1 with β-actin mRNA-containing granules within cell protrusions was observed by in situ hybridization (Fig. 1, E–G). Accumulation of overexpressed GFP–ZBP1 caused partial masking of granular structures. We do not expect to find a total colocalization of β-actin mRNA with GFP–ZBP1 for several reasons. First, there must be some competition between exogenous GFP–ZBP1 and endogenous ZBP1 for β-actin mRNA. Second, it has not been demonstrated that β-actin mRNA is the only cargo of ZBP1. Finally, at some point ZBP1 must dissociate from the RNA after transport to the periphery.

The KH region of ZBP1 mediates granule formation

We expressed several fragments of ZBP1 fused to GFP in CEFs to define which regions of the protein mediate granule formation, cytoskeletal interaction, and granule localization. Only constructs containing the two COOH-terminal KH domains formed granules and interacted with the cytoskeleton (Fig. 3 and Fig. 2, F–K and F′–K′). Removal of the RRM domains did not affect either granule formation or cytoskeleton association (Fig. 2, F′–K′) in this assay; expression of the four KH domains (189–576) resulted in characteristic ZBP1 granule formation. This activity did not require all four of the KH domains, since a construct containing only the third and fourth KH domains (317–576) formed granules. However, granules formed by constructs lacking the RRM domains distribute evenly throughout the cytoplasm. Specifically, truncated ZBP1 (ΔZBP1; 74–576) retained the characteristic distribution of ZBP1-containing granules. A construct only 10 amino acids shorter, ΔZBP1 (84–576), formed granules that did not accumulate at the cell periphery.

Expression of most COOH-terminal deletions, with the exception of ΔZBP1 (1–556), resulted in a loss of granule formation. These constructs yield a diffuse cytoplasmic appearance (Fig. 2, A–E). Only two stained the nucleus, ΔZBP1 (1–179) and ΔZBP1 (195–403) (Fig. 2, A and E). However, these were small fragments of <50 kD and their nuclear presence might be due to passive diffusion through nuclear pores. Except for ΔZBP1 (1–556), all COOH-terminal deletions were extracted upon treatment with Triton X-100 (Fig. 3 and Fig. 2 L).

Removal of the last 54 amino acids of the protein, which disrupts the fourth KH domain, resulted in a loss of granule formation and cytoskeletal retention (Fig. 3). Any construct

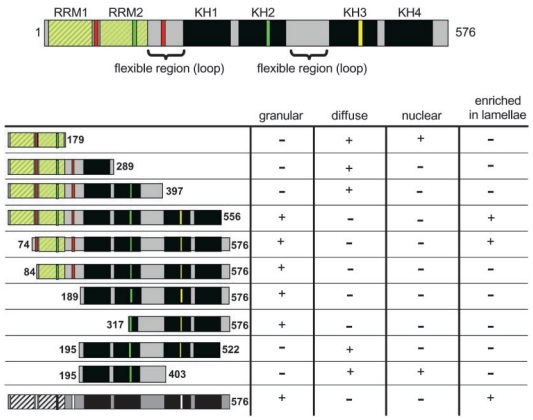

Figure 3. **Localization phenotypes of GFP–ZBP1 deletion mutants.** Red bars indicate putative nuclear localization signals, green bars indicate putative nuclear export signals, and yellow bars indicate putative map kinase sites.

lacking these 54 amino acids, including the construct ΔZBP1 (195–522), appeared diffuse in the cytoplasm. Interestingly, removal of the last 20 amino acids, downstream of the fourth KH domain, did not affect granule formation by the protein and did not affect the localization of the granules in CEFs.

ZBP1 associates with the actin cytoskeleton via KH domains

Cytoskeleton disruption experiments revealed that the cytoskeletal association of ZBP1 was primarily mediated through the actin cytoskeleton. We observed a dramatic loss of ZBP1-containing granules in Triton X-100–extracted cells after treatment with cytochalasin D (Fig. 4, A–C). However, treatment with colchicine resulted in little difference in appearance. In some cases, after microtubule disruption there seemed to be a loss of granules from the perinuclear region of the cytoplasm, whereas granules at the periphery were retained. In contrast, in cells treated with cytochalasin D there were residual granules surrounding the nucleus. Granules could sometimes be detected along microtubule tracks extending out toward the periphery of the cell; ΔGFP–KH1-KH4 (189–576) gave results similar to full-length ZBP1 (Fig. 4, D–F). It remained sensitive to cytochalasin D treatment, indicating that microfilament association is mainly mediated by the COOH-terminal KH domains.

KH domains of ZBP1 specifically bind the zipcode of β-actin mRNA

We examined the ability of various constructs to directly bind the zipcode using both electrophoretic mobility shift assays (Fig. 5, A and B) and filter binding assays (Fig. 5, C and D).

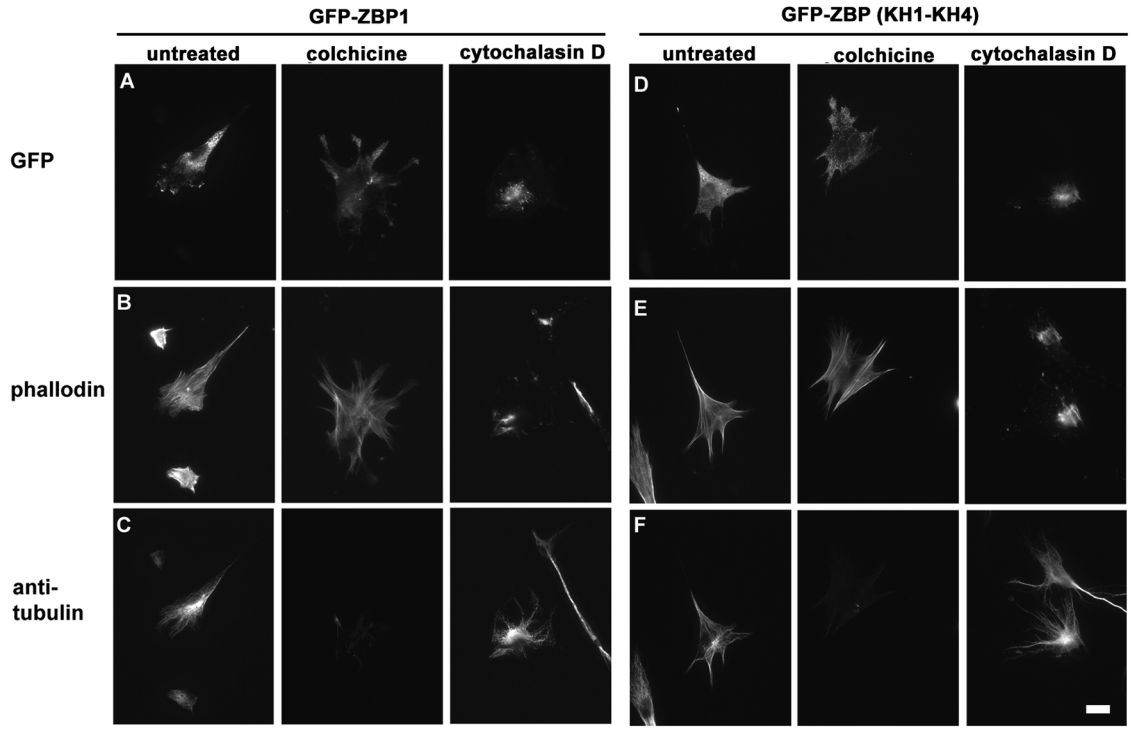

Figure 4. **Anchoring of ZBP1 granules to the actin cytoskeleton is mediated by KH domains.** CEF cells were transfected with GFP-tagged ZBP1 (A–C) or GFP-tagged KH1-KH4 (189–576) (D–F). After treatment with either cytochalasin D or colchicine, cells were Triton extracted, fixed, labeled, and viewed. Localization of GFP proteins on the microfilament (Phalloidin) or microtubule (anti-tubulin) systems was visualized and compared. In colchicine-treated cells, the microtubule system was significantly diminished; however, both GFP-tagged proteins were still associated with granular structures and retained their typical localization compared with untreated cells. In contrast, treatment with cytochalasin D destroyed the microfilament system and caused a significant loss of protein after extraction. Residual granular staining was only observed in the perinuclear region, indicating that granule formation and specific subcellular distribution mediated by the KH domains is mainly based on the actin cytoskeleton.

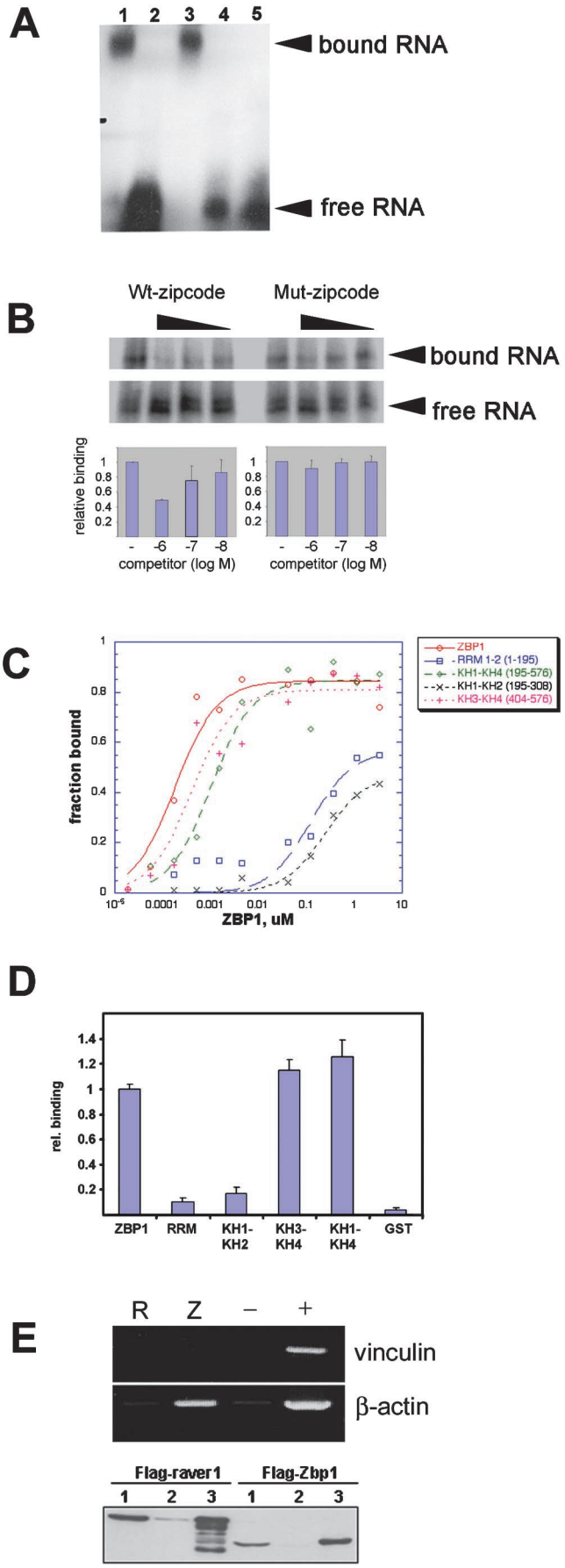

We determined that the region containing the two COOH-terminal KH domains of ZBP1, not the RRM domains, binds the β-actin mRNA zipcode. Recombinant full-length ZBP1 and fragments comprising KH1-KH4 (ΔZBP1 [195–576]) or KH3-KH4 (ΔZBP1 [404–576]) specifically bind the zipcode, whereas fragments comprising only the RRM domains (ΔZBP1 [1–195]) or the first and second KH domains (ΔZBP1 [195–308]) remained inactive (Fig. 5, A, C, and D). Binding by the KH domains showed the same resistance to RNase T1 digestion as full-length ZBP1 (unpublished data). ZBP1 interactions with the zipcode are stable in the presence of excess nonspecific competitor mRNA and in the presence of a mutated zipcode sequence (Fig. 5, A–C). However, excess zipcode mRNA is capable of competing for the labeled zipcode mRNA in the mobility shift assay (Fig. 5 B).

Full-length ZBP1 binds the zipcode with a K_d in the nM range (1–10 nM; Fig. 5 C). The affinities of ΔZBP1 (195–576) and (404–576) for the zipcode were only slightly reduced (approximately threefold) compared with full-length ZBP1. The slightly higher affinity of the full-length may be the result of additional nonspecific binding by the RRM domains or other regions of the protein. The regions of ZBP1 containing the RRM domains (1–179) or KH1-KH2 (195–304) bound the zipcode with ~100-fold less affinity than KH3-KH4.

Figure 5. **The KH domains of ZBP1 specifically bind the zipcode of β-actin mRNA.** (A) Electrophoretic mobility shift assay of ^{32}P-labeled zipcode RNA with recombinant GST–ZBP1 fragments. ZBP1 fragments were incubated with labeled zipcode in the presence of *E. coli* tRNA nonspecific competitor followed by heparin. (Lane 1) ZBP1; (lane 2) RRM1–2 (1–195); (lane 3) KH1-KH4 (195–576); (lane 4) GST; (lane 5) no protein. Note that only the full-length protein and the fragment containing the KH domains (lanes 1 and 3) caused a significant shift of the labeled RNA. No binding was observed for the RRM domains or GST (2 and 4). (B) Interaction between zipcode RNA and ZBP1 was reduced by addition of wild-type zipcode RNA but not by mutated zipcode RNA. (C) Nitrocellulose filter binding assay of recombinant GST–ZBP1 fragment affinity for β-actin mRNA zipcode: ZBP1 (1–576), RRM1-2 (1–195), KH1-KH4 (195–576), KH1-2 (195–308), KH3-KH4 (404–576). Recombinant proteins at various concentrations were incubated with ^{32}P-labeled zipcode RNA. Bound probe was detected by Cerenkov counting after binding of the protein–RNA complex to the filter and intensive washing. All fragments containing at least KH domain 3 and 4 bound the zipcode with a K_d in the nM range. (D) To determine the relative affinities of GST–ZBP1 fragments for full-length β-actin, mRNA binding was analyzed in GST pull-down assays. The fraction of bound ^{32}P-labeled human β-actin RNA retained on equal amounts of immobilized GST–ZBP1 proteins were normalized to binding of full-length ZBP1 and plotted according to the fragments used. All proteins containing at least KH3 and 4 bound the full-length mRNA at apparently equal affinity. (E) Human β-actin mRNA coimmunoprecipitates specifically with Flag-tagged ZBP1. RT-PCR amplification of vinculin or β-actin mRNA extracted from supernatant of nontransfected cells (+) or pellets of FLAG–ZBP1 (Z), FLAG–raver1 (R), or mock (−)-transfected cells after immunoprecipitation with anti-Flag (M2). Human β-actin mRNA was specifically enriched in FLAG–ZBP1 pellets, whereas no enrichment of vinculin mRNA was detected. Precipitation of the FLAG-tagged raver1 (left, bottom) or ZBP1 (right, bottom) was verified by Western blotting of pellet fractions using anti-Flag (M2) antibody. (Lane 1) Total cell extract; (lane 2) supernatant after immunoprecipitation; (lane 3) pelleted fraction.

Figure 6. **Selection of ZBP1 (KH3-KH4) ligands using RNA selection amplification (SELEX).** (A) Lowercase letters are fixed sequences present in RNA library clones. Boxed sequences indicate consensus sequence. (B) Interaction of ZBP1 with zipcode RNA was reduced by addition of 20-mer oligonucleotides that bear ACACCC repeats of the zipcode or consensus SELEX sequences (S1).

Characterization of ZBP1 interactions with full-length human β-actin mRNA was performed with GST pull-down assays (Fig. 5 D). Relative binding affinities of the domains were normalized to that of the full-length protein. KH3-KH4 (404–576) bound full-length human β-actin mRNA with approximately the same relative affinity as full-length ZBP1 or the fragment comprising all four KH domains. No significant binding was observed for KH1-2, the RRM domains, or GST. These observations recapitulated the results obtained for ZBP1 binding to the zipcode.

Binding of ZBP1 to β-actin mRNA in vivo was demonstrated by copurifying endogenous β-actin mRNA with epitope-tagged ZBP1 from human 293 cell extracts (Fig. 5 E, top). As expected from the in vitro analysis, Flag-tagged chicken ZBP1 specifically binds β-actin mRNA in vivo, whereas no binding was observed for vinculin mRNA. Another RNA binding protein, raver1 (Huttelmaier et al., 2001), remained inactive, and no β-actin mRNA was copurified in cells transfected with empty plasmid. ZBP1 and raver1 are present in similar amounts in 293 cell extracts as shown in Fig. 5 E (bottom).

SELEX analysis confirms the zipcode as RNA target of the KH3-KH4 domains

We used RNA selection amplification (SELEX) (Ellington and Szostak, 1990; Tuerk and Gold, 1990) to determine the sequence specificity of the ZBP1 zipcode RNA binding region. For this experiment, we used the deletion construct ΔZBP1 (404–576) in eight rounds of selection amplification. This construct comprises the third and fourth KH domains and the remaining COOH-terminal amino acids of the protein. We chose this construct because it suffices for high affinity zipcode binding in filter binding assays. After eight rounds of selection, the resultant RNA pool was cloned and sequenced. 71% percent of the clones (12 out of 17) could be organized into a strong consensus group (Fig. 6 A). These clones contained the 11-mer 5′-AAGCACCCGTT-3′ or some close variant of this sequence. In addition to the clones that are included in Fig. 6 A, four clones harbored the sequence 5′-CCGCACG-3′ (unpublished data). One clone was quite random and harbored no enrichments. The zipcode of β-actin mRNA, a putative stem-loop, contains repeats of an almost identical element in its predicted loop region, $(5'\text{-ACACCC-}3')_2$ (Kislauskis et al., 1993; Ross et al., 1997). Thus, the ZBP1 KH3-KH4 domains appear to exhibit a preference for the sequence 5′-RCACCC-3′ (R denotes pyrimidine) both in selected ligands and in a physiological ligand. To compare the relative affinities of the ACACCC repeats of the zipcode versus the SELEX consensus sequence for ZBP1, competition experiments were performed with 20-mer oligoribonucleotides containing portions of the zipcode or the SELEX consensus sequence (Fig. 6 B, S1). The SELEX consensus was equally as efficient at competing for binding with ZBP1 as were the zipcode sequences containing ACACCC (Fig. 6 B).

Overexpression of RNA binding domains of ZBP1 results in delocalization of β-actin mRNA

We hypothesized that ZBP1 contains both RNA binding regions and "localizing" regions that support interactions responsible for bringing the RNA and the protein to their ultimate destination. If true, overexpression of the RNA binding region alone should diminish β-actin localization to the lamellae. To investigate this possibility, we transfected CEFs with GFP-fused deletion constructs and examined the percentage of transfected cells in which β-actin mRNA was localized to the leading lamellae. Transfection of GFP–ZBP1 led to an ∼20-fold increase in cellular ZBP1 as measured by mean fluorescent intensity differences between transfected and nontransfected cells immunostained for ZBP1 (unpublished data).

β-Actin mRNA was localized in 40–50% of nontransfected cells and cells transfected with GFP alone (unpublished data). Overexpression of GFP–ZBP1 had no effect on β-actin localization (Fig. 7). Three of the overexpressed constructs decreased β-actin localization by ∼50%: ΔZBP1 (1–289), ΔZBP1 (189–576), and ΔZBP1 (317–576) (Fig. 7). ΔZBP1 (1–289) contains the two RRM domains and the first KH domain. The other two constructs, ΔZBP1 (189–576) and ΔZBP1 (317–576), contain all four KH domains and the two COOH-terminal KH domains, respectively. There was no obvious difference in the delocalization phenotype elicited by each of the dominant-negative constructs (1–289, 189–576, and 317–576). Each caused β-actin mRNA granules to appear evenly distributed throughout the

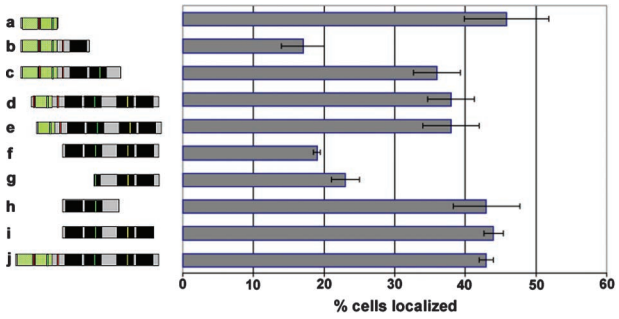

Figure 7. **ZBP1 plays a role in β-actin mRNA localization.** CEFs were transfected with deletion mutants of ZBP1 fused to GFP. Constructs are schematically represented to the left of the table as follows: RRM domains are yellow with green hatching, KH domains are in black, putative nuclear export signal are in green, putative nuclear localization signals are in red, putative MAP kinase site are in yellow. After fixation and permeabilization, in situ hybridization was performed to detect β-actin mRNA. Bars show the percentage of transfected cells counted with β-actin mRNA localized to leading edge. At least 100 cells were counted blind per coverslip in three experiments each. Routinely, 40–50% of nontransfected CEFs show β-actin mRNA localization (unpublished data). (a, 1–179; b, 1–289; c, 1–397; d, 74–576; e, 84–576; f, 189–576; g, 317–576; h, 195–403; i, 195–522; j, 1–576 [ZBP1]).

cytoplasm. Overexpression of the remaining constructs had no effect on β-actin localization in CEFs.

Overexpression of ZBP1 KH domains that delocalize β-actin mRNA also inhibit chick embryo fibroblast motility

β-Actin mRNA localization at the leading edge is required for maintenance of cell polarity and directed cell motion (Kislauskis et al., 1994, 1997). Delocalization of β-actin mRNA by antisense oligonucleotides resulted in delocalized actin nucleation sites and decreased persistence of cell movement (Shestakova et al., 2001). Based on ZBP1's role in β-actin mRNA localization and its presence at the leading edge of CEFs, we predicted that it might also influence cell motility. We tested this possibility directly by transiently overexpressing CEFs with either full-length ZBP1 or β-actin mRNA delocalizing ΔZBP1 (195–576). Movement of the GFP-positive transfected cells was captured by time-lapse videomicroscopy, according to the method of Shestakova et al. (2001). Motility parameters examined include: total path length, net path length, average speed, directionality, persistence, and protrusion velocity (average instantaneous velocity). Of these, total path length, speed, and protrusion velocity were significantly decreased in cells overexpressing the GFP fusions of ZBP1 or ΔZBP1 (189–576) compared with cells expressing GFP alone or nontransfected cells (Table I).

Discussion

In this study, we have characterized structural and functional features of the β-actin mRNA binding protein ZBP1. These data present the first direct evidence for a role of ZBP1 in the localization of β-actin mRNA and consequently in directed fibroblast motility. They begin to elucidate a sequence of events involved in β-actin mRNA localization: (1) ZBP1 binds to the zipcode of β-actin mRNA via its COOH-terminal KH domains, (2) auxiliary factors (e.g., hnRNPs, motors, translational factors) assemble to form a fully functional transport complex (locasome), (3) the locasome associates with the cytoskeleton, (4) the locasome is transported by motors on the cytoskeleton, (5) the locasome anchors at the cell periphery, and (6) the mRNA is translated.

In vitro binding analyses identify the two most COOH-terminal KH domains (KH3-KH4) to be necessary and sufficient for binding the zipcode and the full-length β-actin mRNA. Other RNA binding modules identified within ZBP1 may contribute to protein–RNA complex formation, since slightly lower K_d values were obtained for full-length ZBP1 compared with the KH domains alone. The affinities

Table I. **Overexpression of full-length ZBP1 and dominant-negative ZBP1 (KH1-KH4) alters fibroblast motility**

	Total path length[a]	Net path length[b]	Directionality[c]	Speed	Persistence[d]	Protrusion velocity[e]
	μm	*μm*	*net/total*	*μm/min*	*μm/min × deg*	*μm/min*
GFP	116.65	17.75	0.15	0.30	0.22	1.23
SEM	0.66	0.47	0.00	0.30	0.00	0.01
ZBP1	100.10	15.97	0.15	0.27	0.19	1.04
SEM	0.61	0.35	0.00	0.01	0.00	0.01
Student's *t* test	0.00	0.31	0.36	0.31	0.05	0.00
KH1-KH4	100.33	14.10	0.14	0.23	0.19	1.06
SEM	0.41	0.21	0.00	0.00	0.00	0.01
Student's *t* test	0.00	0.13	0.36	0.13	0.05	0.00
Mock transfection	113.74	18.69	0.16	0.31	0.22	1.22
SEM	0.40	0.24	0.00	0.00	0.00	0.00
Student's *t* test (versus GFP)	0.27	0.32	0.32	0.32	0.27	0.36

[a]Total path length, average of total distance traveled by each cell from start to end point.
[b]Net path length, average distance traveled by each cell between beginning and end point of analyses.
[c]Directionality, net path length/total path length.
[d]Persistence, measurement of directed movement based on number of turns cell makes in degrees per min.
[e]Protrusion velocity, average instantaneous velocity; the average protrusion movement over each 1-min interval.
GFP (n = 35), GFP–ZBP1 (n = 42), ZBP1 (KH1-4) (n = 59), MOCK (n = 88).
SEM, standard error of the mean.

observed for either the RRM domains or the first and second KH domains were significantly lower, suggesting that these domains may contribute to nonspecific mRNA interactions or may bind other specific mRNA sequences. The latter possibility could explain why human ZBP1 (IMP-1) and mouse ZBP1 (CRD-BP) have distinct RNA sequence specificities from chicken ZBP1 (Doyle et al., 1998; Nielsen et al., 1999).

The RNA-binding specificity of KH3-4 is demonstrated by the two ACACCC repeats in the zipcode that are absolutely required for proper localization of the mRNA and for binding to ZBP1 (Kislauskis et al., 1993; Ross et al., 1997). The selection of an RCACCC consensus element by the KH3-KH4 domains in the SELEX experiment strongly agrees with this data. Secondary structure predictions of the zipcode suggest that it forms a stem-loop with $(ACACCC)_2$ in the loop (Ross et al., 1997). These findings indicate that, at least in the context of ZBP1 and the zipcode, the ACACCC region is an important RNA element for binding by KH domains. Such a phenomenon has been reported previously in the case of the KH domain–containing protein Nova, whose third KH domain was shown by biochemical and x-ray crystallographic studies to bind primarily to a UCAY tetranucleotide element in the loop region of a stem-loop RNA target identified by SELEX (Jensen et al., 2000; Lewis et al., 2000). Our results do not rule out the possibility that there are additional RNA sequences, either within the zipcode itself or within the full-length β-actin mRNA, that are involved in the interaction between ZBP1 and β-actin mRNA.

Full-length ZBP1 and all fragments that contained intact KH3-4 domains were capable of forming granules that were resistant to detergent extraction before fixation, suggesting a direct or indirect link to the cytoskeleton. Based on the mRNA binding properties of ZBP1, these findings strongly suggest that ZBP1 bound to a specific mRNA target assembles into mRNP complexes that associate with the cytoskeleton. This was confirmed by the fact that all COOH-terminal deletion fragments, in which KH3 and KH4 were either completely or partially deleted, showed a diffuse distribution and were extractable with nonionic detergent. Further analysis demonstrated the importance of the structural integrity of the last KH domain. ΔZBP1(1–522), which contains a partially truncated KH4 domain, showed a diffuse distribution, whereas ΔZBP1(1–556) in which the KH4 remained intact formed detergent resistant granules. Together these findings demonstrate that the last two KH domains are sufficient for binding the β-actin mRNA and for assembly into mRNPs that associate with the cytoskeleton. Recently, it has been shown that the third and fourth KH domains of the *Xenopus* homologue of ZBP1, Vg1RBP, mediate self association (Git and Standart, 2002). ZBP1 has also been shown to oligomerize via its KH domains (unpublished data), and this property may be a factor in our observations.

Cytoskeleton disruption experiments showed that in primary fibroblasts ZBP1 granules associate mainly with the actin cytoskeleton. Furthermore, the KH domains of ZBP1 were sufficient to maintain this interaction. These findings are consistent with previous observations that β-actin mRNA localization in fibroblasts is a predominantly actin-based process (Sundell and Singer, 1991; Kislauskis et al., 1993). Although there have been other observations of actin-based RNA localization (Hill and Gunning, 1993; Broadus and Doe, 1997; Long et al., 2000), the majority of localized RNAs described to date are transported via the microtubule cytoskeleton (Elisha et al., 1995; Carson et al., 1997; Bassell et al., 1998; Havin et al., 1998; Wilkie and Davis, 2001). Long distance transport of β-actin mRNA, such as that in neurons, seems to be more dependent on microtubules (Zhang et al., 2001a), whereas short distance transport and anchoring is believed to rely on microfilaments. Since both systems use ZBP1, it may be a universal linker to either myosin or microtubule-based motors.

Although the motor proteins involved in ZBP1 granule transport remain to be identified, the data presented provide insight as to the mechanism by which ZBP1 connects to the transport machinery. Efficient ZBP1 granule localization to the cell periphery depends on the NH_2-terminal part of ZBP1 containing the RRM domains. Granules formed by most constructs lacking the NH_2 terminus were evenly distributed throughout the cytoplasm. We suggest that nonlocalized ZBP1 granules represent localization "incompetent" granules. Presumably, the ZBP1 constructs present in these granules are capable of interacting with the RNA but lack key components necessary for distributing the locasome to the cell periphery. Mislocalization of these granules may be due to defects in targeting, transport, or peripheral anchoring. Similar observations were made for the COOH-terminal KH domains of the human ortholog of ZBP1, IMP1, which formed "immobile aggregates" in NIH-3T3 cells (Nielsen et al., 2002). Similarly, overexpression of the RNA binding domain of Staufen (Stau-RBD) alone resulted in inefficient dendritic localization of Stau-RBD granules (Tang et al., 2001). Together these findings point to a common mechanism where the protein–RNA complex provides a scaffold for mRNP transport. A finer analysis of the NH_2 terminus of ZBP1 indicated that 10 amino acids that lie between the two RRM domains (ΔZBP1 [74–576] versus ΔZBP1 [84–576]) enable ZBP1 granule localization. Whether this 10 amino acid region contributes to the overall stability of a critical secondary structure or whether a specific element in that sequence is responsible for granule localization remains to be determined.

ZBP1 and its homologues associate with a variety of localized transcripts (Deshler et al., 1997; Mueller-Pillasch et al., 1997; Ross et al., 1997; Doyle et al., 1998; Havin et al., 1998; Nielsen et al., 1999; Zhang et al., 1999a, 2001a). However, conclusive evidence indicating that RNA regulation is a direct result of the function of ZBP1 and its family members is not well documented. A recent publication provides evidence of the role of Vg1RBP in the localization of *Vg1* mRNA (Kwon et al., 2002). However, experimental limitations have made it difficult to prove that the function of these RNA binding proteins is actually required for RNA localization to occur. The data presented here demonstrates that overexpression of the zipcode binding region of ZBP1 (KH1-KH4) and (KH3-KH4) significantly delocalizes β-actin mRNA. Based on the high affinity binding of the KH domains to β-actin mRNA, these overexpressed deletion fragments likely suppress mRNA localization by competing with the endogenous ZBP1 for β-actin. Since the COOH-termi-

nal fragments do not localize, mRNA is sequestered within localization "incompetent" granules.

Interestingly, one NH_2-terminal fragment, ΔZBP1 (1–289), delocalizes β-actin mRNA. Although this construct does not bind the zipcode, since it lacks KH3 and KH4, it might still bind to auxiliary factors that are essential for proper localization of ZBP1-containing granules. Thus, overexpression of this construct may suppress proper mRNA localization by competing with endogenous ZBP1 for these essential factors preventing β-actin transcripts bound to endogenous ZBP1 from being properly localized.

Together these findings confirm ZBP1 as an essential factor for localizing β-actin mRNA to the cell periphery. The data presented suggest that ZBP1 not only binds the mRNA via its COOH-terminal KH domains but also tethers the RNA to auxiliary factors via its NH_2 terminus that are required for proper localization of the ZBP1 containing mRNPs.

This model also provides an explanation for the finding that ZBP1 is involved not only in β-actin mRNA localization but also contributes to the regulation of fibroblast motility. Overexpression of either ZBP1 or the COOH-terminal β-actin delocalizing construct ZBP1 (aa 189–576) decreased total path length, cell speed, and protrusion velocity of CEFs. Shestakova et al. (2001) demonstrated that CEFs treated with antisense oligonucleotides, which disrupt β-actin mRNA localization, moved with reduced net path length, directionality, and persistence. Furthermore, this motility phenotype was attributed to delocalized actin nucleation sites resulting from antisense treatment.

These results may seem to be discordant with the current study. However, antisense oligonucleotides were specific for the zipcode of β-actin mRNA and specifically disrupt ZBP1–β-actin mRNA interactions (Zhang et al., 2001a; Oleynikov and Singer, 2003). Therefore, the RNA was freed from any spatial or regulatory constraints due to its interaction with ZBP1. In contrast, in the experiments reported here the interaction of the mRNA with ZBP1 is maintained. This may result in different physiological consequences. For example, localized RNAs are believed to be translationally repressed during transport; the human ortholog of ZBP1, IMP-1, translationally represses insulin-like growth factor II mRNA during fetal development (Nielsen et al., 1999). In contrast to β-actin mRNA delocalized by antisense (Kislauskis et al., 1997; Shestakova et al., 2001), which is free to translate in an unregulated manner, β-actin mRNA bound to ZBP1 may be translationally repressed. Therefore, random actin nucleation may occur as a result of free cytoplasmic β-actin mRNA but not as a result of translationally repressed, ZBP1-bound RNA. Consequently, motility phenotypes described in our experiments fit with a model where there is decreased β-actin protein synthesis at the leading edge, resulting in decreased motility and protrusion rates.

It is important to consider that the physiological effects of both β-actin mRNA localization and ZBP1 function and the mechanism of β-actin mRNA localization are not completely understood at this time. Furthermore, it has not been established that β-actin mRNA is the only RNA target of ZBP1. Thus, a dominant-negative ZBP1 might affect additional mRNAs, causing a broader impact on cell polarity and motility than the results seen by antisense for β-actin mRNA. Additionally, ZBP1 has been implicated in several processes of RNA metabolism besides localization. Therefore, it is difficult to distinguish which aspects of ZBP1, motility regulation, and mRNA localization are being targeted in these experiments. As a result, although β-actin mRNA localization and ZBP1 function are involved in the regulation of cell motility, predictions about how these effects are mediated await further experiments.

Materials and methods

Cell culture and transfection

CEFs were transfected with LT1 reagent (Mirus), according to manufacturer's instructions, at the time of plating. All transfections took place in DME supplemented with 10% FBS. Cells were transfected overnight, washed in Hanks balanced salt solution (HBSS) and recovered in fresh DME plus 10% FBS for 1 h. For serum-starved cells, after 1 h recovery in medium plus serum cells were washed in HBSS and incubated for 4 h in DME. Cells were serum stimulated with fresh DME plus FBS for 30 min followed by fixation in 4% PFA in PBS/5 mM $MgCl_2$. Triton-extracted cells were incubated in 0.5% Triton X-100 for 15 s before fixation. For time-lapse extraction, cells were plated on 35-mm tissue culture plates and transfected as described. After transfection and recovery, MEM plus FBS was replaced with 1 ml Leibovitz's L15 medium without phenol red (Lifetech). Cells were visualized on an Olympus AX70 microscope and 60× water immersion objective. Triton X-100 was added to a final volume of 0.5% Triton X-100.

Immunostaining

After fixation, cells were washed three times for 10 min in 1× PBS/5 mM $MgCl_2$, blocked for 20 min in PBSAT (PBS, 2% BSA, 0.1% Triton X-100), and incubated in primary antibody (1:2,000 in PBSAT) for 1 h at RT. Cells were washed three times for 10 min in PBSAT. Secondary antibody (rabbit anti–mouse antibody, 1:250 in PBSAT [Jackson ImmunoResearch Laboratories]) was applied for 20 min at RT. Cells were washed once for 10 min in PBSAT, twice for 10 min in PBS, and mounted on glass slides in ProLong antifade mounting media (Molecular Probes).

Fluorescent in situ hybridization

Fixed cells were hybridized with a mixture of six Cy-3–labeled oligonucleotides complementary to β-actin mRNA for 3 h in 50% formamide/2× SSC at 37°C. Cells were washed and mounted on glass slides. Cells were scored blinded for localization as previously described (Kislauskis et al., 1994; Latham et al., 1994).

Cytoskeleton disruption experiment

After transfection, cells were recovered in MEM plus 10% FBS for 4 h. Either cytochalasin D (5 μg/ml; Sigma-Aldrich) or colchicine (100 μM; Sigma-Aldrich) was added to the medium for 30 min. Cells were washed briefly in PEM buffer (100 mM PIPES, 2 mM EGTA, 10 mM KCl, 10% glycerol) warmed to 37°C and then extracted for 20 s in warm PEM buffer plus 0.5% Triton X-100. Cells were fixed for 15 min in 4% paraformaldehyde/PEM buffer. Microtubules were immunostained with DM1α antitubulin antibody (Sigma-Aldrich). Secondary antibody (Cy5-conjugated rabbit anti–mouse antibody, 1:250 in PBSAT [Jackson ImmunoResearch Laboratories]) and Texas red phalloidin (Molecular Probes) were applied for 20 min at RT. Cells were washed once for 10 min in PBSAT, twice for 10 min in PBS, and mounted on glass slides in ProLong antifade mounting medium (Molecular Probes).

Microscopy

Cells were viewed on either an Olympus BX60 or BX51 microscope equipped with an Olympus PlanApo 60×, 1.4 NA oil objective. Images were captured with either an LSR FKI1001 or a Roper CoolSNAP HQ cooled CCD camera operated by LSR Esprit v4.0 or Scanalytics IP Lab Windows v3.0.72, respectively.

Recombinant protein expression

ZBP1 and its domains were amplified by PCR (ZBP1 aa: 1–576, 1–195, 195–576, 195–348, 404–576), sequenced, and inserted into EcoRI-XhoI sites of pGEX6P1 vector (Amersham Biosciences). Protein expression was induced in *Escherichia coli* BL21(DE3) cells with 1 mM IPTG. Purification

was performed according to manufacturer's protocol with slight modifications. Briefly, bacteria were lysed in lysis buffer (PBS, 0.1% Triton X-100, 1 mM DTT, 500 mM NaCl) supplemented with protease inhibitors and lysozyme. After sonification and clearing of the cell lysate at 30,000 *g*, the cell extracts were incubated with glutathione–Sepharose for 1 h at 4°C. After extensive washing with lysis buffer, proteins were eluted in storage buffer (PBS, 150 mM NaCl, 2% glycerol, 2 mM DTT) supplemented with 20 mM reduced glutathione. Proteins were desalted into storage buffer via PD-10 columns (Amersham Biosciences) and stored at 4°C for immediate use. Protein concentrations were determined by Coomassie blue staining of SDS–polyacrylamide gels and by Bradford assay. Proteins were used only if purity >90% was confirmed by SDS-PAGE.

In vitro transcription

For electrophoretic mobility shift assays and nitrocellulose filter binding assays, the 54-nt β-actin zipcode RNA was randomly labeled with [α-^{32}P]CTP (Amersham Biosciences) during in vitro SP6 polymerase transcription from a linearized template (pSP64 plasmid; Promega). In vitro transcription was performed with a Promega RiboProbe Kit according to manufacturer's instructions. Probes were urea gel purified and resuspended at a concentration of 10,000 cpm/μl in diethylpyrocarbonate (DEPC)–treated water.

For GST pull-down assays, full-length human β-actin mRNA was subcloned into pcDNA3.1 (Invitrogen) and transcribed in the presence of [α-^{32}P]UTP (Amersham Biosciences) after linearization by XhoI via the T7 Megascript kit (Ambion). RNA was purified by MegaClear (Ambion) and analyzed by 5% TBE/Urea gels (Bio-Rad Laboratories).

RNA binding studies

Electrophoretic mobility shift assay. Binding reactions contained the following: 10 mM Tris, pH 7.5, 50 mM NaCl, 1 mM $MgCl_2$, 0.5 mM EDTA, 0.5 mM DTT, 4% glycerol, and 0.25 mg/ml poly (dI-dC), 10,000 cpm labeled zipcode RNA, and 500 ng recombinant protein to a final volume of 20 μl. *E. coli* tRNA (Roche) was added at a final concentration of 5 mg/ml in reactions performed in the presence of nonspecific competitor. Reactions were incubated for 30 min at RT. Heparin sulfate was added to a final concentration of 5 mg/ml followed by a 10-min incubation. Reactions were loaded on 5% nondenaturing polyacrylamide TGE gel containing 5% glycerol. In competition assays, cold wild-type zipcode RNA or mutant zipcode (ACACCC repeats replaced by GUGUGU) RNA were incubated with 50 ng protein for 10 min at RT followed by addition of ^{32}P-labeled zipcode RNA. Unlabeled RNA was added at 400×, 40×, and 4× excess over labeled zipcode. After electrophoresis, gels were fixed in 10% isopropanol/7% acetic acid for 15 min, dried, and exposed to autoradiography film or phosphoimager cassette. Signal intensities were measured with ImageQuant software (Molecular Dynamics). Relative binding indicates the fraction of total counts bound by protein.

Nitrocellulose filter binding assay. Filter binding assays (Carey et al., 1983) were used to measure the binding dissociation constants between the zipcode mRNA and ZBP1 recombinant protein fragments. 50 μl binding reactions contained the following: 200 mM KOAc, 50 mM Tris acetate (pH 7.7), 5 mM MgOAc, 10,000 cpm labeled zipcode RNA, and threefold serially diluted recombinant ZBP1 protein fragments ranging from 40 to 50 nM. Reactions were incubated for 10 min at RT followed by filtering (Millipore HAWP 25 mm filter/1225 Sampling Manifold) and washing. The fraction of bound RNA was plotted graphically versus the log of protein concentration to determine dissociation constants (Irvine et al., 1991). For competition assays, labeled and unlabeled RNA oligonucleotides (Z1, 5′-CCAACACCCACACCCCUGUG-3′; Z2, 5′-CUGUGAUGAAACAAAACCCA-3′; Z3, 5′-GAAACAAAACCCAUAAAUGC-3′; and S1, 5′-AAGCACCCGUUUCAGUACGC-3′) were incubated at RT for 10 min followed by addition of protein.

GST pull-down assays. GST proteins were adjusted to a final concentration of 0.25–0.5 μM in 350 uL ice cold RBB (PBS, 2 mM $MgCl_2$, 0.02% NP-40, 0.1% BSA, 1 mM DTT, 50 U/ml RNAsin) and incubated for 1 h at 4°C with 50 uL of a 1:1 slurry of glutathione–Sepharose (Amersham Biosciences) preblocked with 1% BSA in RBB. The resin was washed four times and labeled, and renatured β-actin mRNA (~100,000 cpm, 5–10 fmol) was added in a final volume of 100 μL. After incubation for 30 min at 4°C, the resin was washed two times with RWB (10 mM Tris, pH 8.0, 150 mM NaCl, 2 mM $MgCl_2$, 0.1% NP-40, 1 mM DTT). Resin was transferred to a new tube and washed. Aliquots of wash fractions and pellet fractions were analyzed by Cerenkov counting.

Immunoprecipitation and RT-PCR. Human 293 cells were transfected with Flag-tagged ZBP1 or raver1 constructs or empty pcDNA3.1 plasmid (mock transfection). Cells were extracted in IP/RT buffer (50 mM Tris/HCl, pH 8.0, 150 mM KCl, 1 mM EGTA, 5 mM $MgCl_2$, 0.25% NP-40, 0.05% DOC, 100 U/ml RNAsin) for 30 min on ice. Extracts were centrifuged at 14,000 rpm for 15 min, and supernatants were subjected to immunoprecipitation using anti-Flag M2-agarose beads (Sigma-Aldrich) for 1–2 h. Beads were washed three times with IP/RT buffer, and after removing the final wash fraction RNA–protein was eluted by boiling the beads in 200 μl DEPC-treated water. All fractions were collected for Western blot analysis using anti-Raver and anti-ZBP1 antibodies to determine relative protein quantities. RNA was recovered using Trizol reagent (Gibco Life Technologies) according to the manufacturer's protocol and resuspended in 20 μl DEPC-treated water. For reverse transcription, the One step RT-PCR kit from QIAGEN was used. The following primers were used for amplification: *human β-actin* (s, 5′-AAAACCTAACTTGCGCAGAAAACA-3′; r, 5′-GGGCACGAAGGCTCATCATT-3′); *human vinculin* (s, 5′-CTAGGCAAAATGAGAGGGCAGTGT-3′; r, 5′- CATCCGGCATAAAGTGTAAACCAGTG-3′).

SELEX experiment. Recombinant ZBP1 (404–576) protein spanning KH3-KH4 was subjected to RNA selection amplification. The synthetic oligonucleotide templates 5′-TCCCGCTCGTCGTCT [40N] CCGCATCGTCCTCCCT-3′, where N indicates random incorporation of all four nucleotides, were prepared for first round transcription by using Klenow fragment (Amersham Biosciences) and the oligonucleotide primer 5GL, 5′-GAAATTAATACGACTCACTATAGGGAGGACGATGCGG-3′. Each template was transcribed with recombinant T7 polymerase (Stratagene) to yield several nmol of full-length product, which was size purified with 10% denaturing PAGE and used for first round selection. Selection amplification was performed essentially as described by Tuerk and Gold (1990) and Jensen et al. (2000). Briefly, protein–RNA binding reactions were performed in buffer SBB (200 mM KOAc, 5 mM $Mg[OAc]_2$, 50 mM Tris-OAc, pH 7.7) using an excess of RNA to protein, and partitioning was performed with 0.45 μM pore size nitrocellulose filters (Millipore). Selected RNA was extracted from filters with urea/phenol/chloroform treatment and reverse transcribed with the oligonucleotide primer 3GL, 5′-TCCCGCTCGTCGTCTG-3′, and AMV-RT (Promega). PCR amplification of the selected clones for subsequent rounds of transcription and selection used mildly mutagenic conditions with primers 5GL and 3GL, 1 mM dNTPs, and 7.5 mM $Mg(OAc)_2$. All oligonucleotides were from Operon.

Motion analysis

CEFs (10^6) were plated on 35-mm tissue culture plates coated with 0.5% gelatin and transfected in α-MEM medium supplemented with 10% FBS/1% Pen-Strep. Cells were recovered for 1 h in L15 medium supplemented with 10% FBS/1% Pen-Strep (Life Technologies). Videomicroscopy was performed on an Olympus microscope equipped with a cooled CCD camera using IP Lab Software. Phase images at 10× were captured at 1-min intervals for 1 h. Cells were traced with Scion image software and converted to digitized movies. Cell centroids and motility parameters were computed using DIAS software (Solltech). Detailed explanation of motility parameters described in Soll (1995). Student *t* tests were performed by comparing each dataset to GFP-transfected cell data.

We would like to thank Yuri Oleynikov for his valuable contributions, Shailesh Shenoy, Mark Francescone, Michael Cammer, Jeff Wyckoff, and the staff of the Analytical Imaging Facility for help with imaging and motion analysis, Feng Pan for critical reading of the manuscript, Steven Braut for technical assistance, and our colleague Stephen Burley for his help and support.

This work was supported by National Institutes of Health grant AR41480 to R.H. Singer.

Submitted: 3 June 2002
Revised: 22 November 2002
Accepted: 25 November 2002

References

Barbarese, E., D.E. Koppel, M.P. Deutscher, C.L. Smith, K. Ainger, F. Morgan, and J.H. Carson. 1995. Protein translation components are colocalized in granules in oligodendrocytes. *J. Cell Sci.* 108:2781–2790.

Bashirullah, A., R.L. Cooperstock, and H.D. Lipshitz. 1998. RNA localization in development. *Annu. Rev. Biochem.* 67:335–394.

Bassell, G.J., H. Zhang, A.L. Byrd, A.M. Femino, R.H. Singer, K.L. Taneja, L.M. Lifshitz, I.M. Herman, and K.S. Kosik. 1998. Sorting of beta-actin mRNA and protein to neurites and growth cones in culture. *J. Neurosci.* 18:251–265.

Broadus, J., and C.Q. Doe. 1997. Extrinsic cues, intrinsic cues and microfilaments regulate asymmetric protein localization in *Drosophila* neuroblasts. *Curr. Biol.* 7:827–835.

Carey, J., V. Cameron, P.L. de Haseth, and O.C. Uhlenbeck. 1983. Sequence-specific interaction of R17 coat protein with its ribonucleic acid binding site. *Biochemistry.* 22:2601–2610.

Carson, J.H., K. Worboys, K. Ainger, and E. Barbarese. 1997. Translocation of myelin basic protein mRNA in oligodendrocytes requires microtubules and kinesin. *Cell Motil. Cytoskeleton.* 38:318–328.

Deshler, J.O., M.I. Highett, and B.J. Schnapp. 1997. Localization of *Xenopus* Vg1 mRNA by Vera protein and the endoplasmic reticulum. *Science.* 276:1128–1131.

Deshler, J.O., M.I. Highett, T. Abramson, and B.J. Schnapp. 1998. A highly conserved RNA-binding protein for cytoplasmic mRNA localization in vertebrates. *Curr. Biol.* 8:489–496.

Doyle, G.A., N.A. Betz, P.F. Leeds, A.J. Fleisig, R.D. Prokipcak, and J. Ross. 1998. The c-myc coding region determinant-binding protein: a member of a family of KH domain RNA-binding proteins. *Nucleic Acids Res.* 26:5036–5044.

Elisha, Z., L. Havin, I. Ringel, and J.K. Yisraeli. 1995. Vg1 RNA binding protein mediates the association of Vg1 RNA with microtubules in *Xenopus* oocytes. *EMBO J.* 14:5109–5114.

Ellington, A.D., and J.W. Szostak. 1990. In vitro selection of RNA molecules that bind specific ligands. *Nature.* 346:818–822.

Git, A., and N. Standart. 2002. The KH domains of *Xenopus* Vg1RBP mediate RNA binding and self-association. *RNA.* 8:1319–1333.

Havin, L., A. Git, Z. Elisha, F. Oberman, K. Yaniv, S.P. Schwartz, N. Standart, and J.K. Yisraeli. 1998. RNA-binding protein conserved in both microtubule- and microfilament-based RNA localization. *Genes Dev.* 12:1593–1598.

Hill, M.A., and P. Gunning. 1993. Beta and gamma actin mRNAs are differentially located within myoblasts. *J. Cell Biol.* 122:825–832.

Huttelmaier, S., S. Illenberger, I. Grosheva, M. Rudiger, R.H. Singer, and B.M. Jockusch. 2001. Raver1, a dual compartment protein, is a ligand for PTB/hnRNPI and microfilament attachment proteins. *J. Cell Biol.* 155:775–786.

Irvine, D., C. Tuerk, and L. Gold. 1991. SELEXION. Systematic evolution of ligands by exponential enrichment with integrated optimization by non-linear analysis. *J. Mol. Biol.* 222:739–761.

Jensen, K.B., K. Musunuru, H.A. Lewis, S.K. Burley, and R.B. Darnell. 2000. The tetranucleotide UCAY directs the specific recognition of RNA by the Nova K-homology 3 domain. *Proc. Natl. Acad. Sci. USA.* 97:5740–5745.

King, M.L., Y. Zhou, and M. Bubunenko. 1999. Polarizing genetic information in the egg: RNA localization in the frog oocyte. *Bioessays.* 21:546–557.

Kislauskis, E.H., Z. Li, R.H. Singer, and K.L. Taneja. 1993. Isoform-specific 3′-untranslated sequences sort alpha-cardiac and beta-cytoplasmic actin messenger RNAs to different cytoplasmic compartments. *J. Cell Biol.* 123:165–172.

Kislauskis, E.H., X. Zhu, and R.H. Singer. 1994. Sequences responsible for intracellular localization of beta-actin messenger RNA also affect cell phenotype. *J. Cell Biol.* 127:441–451.

Kislauskis, E.H., X. Zhu, and R.H. Singer. 1997. beta-Actin messenger RNA localization and protein synthesis augment cell motility. *J. Cell Biol.* 136:1263–1270.

Kloc, M., N.R. Zearfoss, and L.D. Etkin. 2002. Mechanisms of subcellular mRNA localization. *Cell.* 108:533–544.

Kwon, S., T. Abramson, T.P. Munro, C.M. John, M. Kohrmann, and B.J. Schnapp. 2002. UUCAC- and Vera-dependent localization of VegT RNA in *Xenopus* oocytes. *Curr. Biol.* 12:558–564.

Lasko, P. 2000. The *Drosophila* melanogaster genome: translation factors and RNA binding proteins. *J. Cell Biol.* 150:F51–F56.

Latham, V.M., Jr., E.H. Kislauskis, R.H. Singer, and A.F. Ross. 1994. Beta-actin mRNA localization is regulated by signal transduction mechanisms. *J. Cell Biol.* 126:1211–1219.

Lawrence, J.B., and R.H. Singer. 1986. Intracellular localization of messenger RNAs for cytoskeletal proteins. *Cell.* 45:407–415.

Leeds, P., B.T. Kren, J.M. Boylan, N.A. Betz, C.J. Steer, P.A. Gruppuso, and J. Ross. 1997. Developmental regulation of CRD-BP, an RNA-binding protein that stabilizes c-myc mRNA in vitro. *Oncogene.* 14:1279–1286.

Lewis, H.A., K. Musunuru, K.B. Jensen, C. Edo, H. Chen, R.B. Darnell, and S.K. Burley. 2000. Sequence-specific RNA binding by a Nova KH domain: implications for paraneoplastic disease and the fragile X syndrome. *Cell.* 100:323–332.

Long, R.M., R.H. Singer, X. Meng, I. Gonzalez, K. Nasmyth, and R.P. Jansen. 1997. Mating type switching in yeast controlled by asymmetric localization of ASH1 mRNA. *Science.* 277:383–387.

Long, R.M., W. Gu, E. Lorimer, R.H. Singer, and P. Chartrand. 2000. She2p is a novel RNA-binding protein that recruits the Myo4p-She3p complex to ASH1 mRNA. *EMBO J.* 19:6592–6601.

Mowry, K.L., and C.A. Cote. 1999. RNA sorting in *Xenopus* oocytes and embryos. *FASEB J.* 13:435–445.

Mueller-Pillasch, F., U. Lacher, C. Wallrapp, A. Micha, F. Zimmerhackl, H. Hameister, G. Varga, H. Friess, M. Buchler, H.G. Beger, et al. 1997. Cloning of a gene highly overexpressed in cancer coding for a novel KH-domain containing protein. *Oncogene.* 14:2729–2733.

Nielsen, J., J. Christiansen, J. Lykke-Andersen, A.H. Johnsen, U.M. Wewer, and F.C. Nielsen. 1999. A family of insulin-like growth factor II mRNA-binding proteins represses translation in late development. *Mol. Cell. Biol.* 19:1262–1270.

Nielsen, J., F. Cilius Nielsen, R. Kragh Jakobsen, and J. Christiansen. 2000. The biphasic expression of IMP/Vg1-RBP is conserved between vertebrates and *Drosophila*. *Mech. Dev.* 96:129–132.

Nielsen, F.C., J. Nielsen, M.A. Kristensen, G. Koch, and J. Christiansen. 2002. Cytoplasmic trafficking of IGF-II mRNA-binding protein by conserved KH domains. *J. Cell Sci.* 115:2087–2097.

Oleynikov, Y., and R.H. Singer. 2003. Real-time visualization of ZBP1 association with β-actin mRNA during transcription and localization. *Curr. Biol.* In press.

Ross, A.F., Y. Oleynikov, E.H. Kislauskis, K.L. Taneja, and R.H. Singer. 1997. Characterization of a beta-actin mRNA zipcode-binding protein. *Mol. Cell. Biol.* 17:2158–2165.

Shestakova, E.A., J. Wyckoff, J. Jones, R.H. Singer, and J. Condeelis. 1999. Correlation of beta-actin messenger RNA localization with metastatic potential in rat adenocarcinoma cell lines. *Cancer Res.* 59:1202–1205.

Shestakova, E.A., R.H. Singer, and J. Condeelis. 2001. The physiological significance of beta-actin mRNA localization in determining cell polarity and directional motility. *Proc. Natl. Acad. Sci. USA.* 98:7045–7050.

Soll, D.R. 1995. The use of computers in understanding how animal cells crawl. *Int. Rev. Cytol.* 163:43–104.

Steward, O. 1997. mRNA localization in neurons: a multipurpose mechanism? *Neuron.* 18:9–12.

Sundell, C.L., and R.H. Singer. 1991. Requirement of microfilaments in sorting of actin messenger RNA. *Science.* 253:1275–1277.

Tang, SJ., D. Meulmans, L. Vazquez, N. Colaco, and E. Schuman. 2001. A role for a rat homolog of staufen in the transport of RNA to neuronal dendrites. *Neuron.* 32:463–475.

Tuerk, C., and L. Gold. 1990. Systematic evolution of ligands by exponential enrichment: RNA ligands to bacteriophage T4 DNA polymerase. *Science.* 249:505–510.

Wilkie, G.S., and I. Davis. 2001. *Drosophila* wingless and pair-rule transcripts localize apically by dynein-mediated transport of RNA particles. *Cell.* 105:209–219.

Zhang, H.L., R.H. Singer, and G.J. Bassell. 1999a. Neurotrophin regulation of beta-actin mRNA and protein localization within growth cones. *J. Cell Biol.* 147:59–70.

Zhang, J.Y., E.K. Chan, X.X. Peng, and E.M. Tan. 1999b. A novel cytoplasmic protein with RNA-binding motifs is an autoantigen in human hepatocellular carcinoma. *J. Exp. Med.* 189:1101–1110.

Zhang, H.L., T. Eom, Y. Oleynikov, S.M. Shenoy, D.A. Liebelt, J.B. Dictenberg, R.H. Singer, and G.J. Bassell. 2001a. Neurotrophin-induced transport of a beta-actin mRNP complex increases beta-actin levels and stimulates growth cone motility. *Neuron.* 31:261–275.

Zhang, J.Y., E.K. Chan, X.X. Peng, M. Lu, X. Wang, F. Mueller, and E.M. Tan. 2001b. Autoimmune responses to mRNA binding proteins p62 and Koc in diverse malignancies. *Clin. Immunol.* 100:149–156.